Copy No. _____

Defence Research and Development Canada
Recherche et développement pour la défense Canada

DEFENCE R&D DÉFENSE

Ductile to Brittle Transition Behaviour of HSLA-65 Steel Welds

Dynamic Tear Testing

Neil Aucoin

Defence R&D Canada – Atlantic

Technical Memorandum
DRDC Atlantic TM 2010-220
January 2011

Canada

This page intentionally left blank.

Ductile to Brittle Transition Behaviour of HSLA-65 Steel Welds

Dynamic Tear Testing

Neil Aucoin

Defence R&D Canada – Atlantic

Technical Memorandum
DRDC Atlantic TM 2010-220
January 2011

Principal Author

Original signed by Neil Aucoin

Neil Aucoin

Mechanical Engineer

Approved by

Original signed by Terry Foster

Terry Foster

H/DLP

Approved for release by

Original signed by Ron Kuwahara for

Calvin Hyatt

Chair DRP

Abstract

HSLA-65 steel (ASTM A945, grade 65 [1]) is regarded as an excellent naval ship steel. The use of this steel in future naval platforms, which may be required to serve in Arctic conditions, requires a detailed knowledge of the steel's low temperature mechanical properties, particularly when the steel is welded. A previous study on the transition temperature, conducted by Bayley and Mantei [2], showed that the transition temperature was significantly higher than the requirement of -40°C in the heat affected zone of flux-cored arc welding (FCAW) welds.

The current study re-examines the transition behaviour of HSLA-65 welds using dynamic tear testing, where specimens are significantly larger than in Charpy tests and could more accurately predict the behaviour of large scale structures. The current study also examines an alternate approach for determining the energy absorbed during a dynamic tear test using the integral definition of work.

The results of this study show that transition temperatures determined through dynamic tear testing are much higher than those determined through Charpy impact testing. Several areas of each weld were tested. In all cases, the fusion line of the weld was found to have the highest transition temperature, the heat affected zone was found to have the lowest transition temperature, and the weld metal fell somewhere in between. Based on a transition temperature requirement of less than -40°C, none of the welds tested was found to be fit for service in Arctic conditions.

Résumé

L’acier HSLA-65 (acier à haute résistance mécanique) (ASTM A945, nuance 65 [1]) est considéré comme un acier pour bâtiment naval d’excellente qualité. L’utilisation de cet acier dans les plateformes navales futures, qui pourraient être utilisées dans des conditions arctiques, exige une connaissance détaillée des propriétés mécaniques de l’acier à basse température, particulièrement lorsque l’acier est soudé. Une étude antérieure sur la température de transition, réalisée par Bayley et Mantei [2], a montré que la température de transition était beaucoup plus élevée que l’exigence de -40°C dans la zone affectée par la chaleur des soudures réalisées à l’aide du procédé *FCAW* (de l’anglais *Flux-Cored Arc Welding*, ou soudage à l’arc avec fil fourré).

L’étude actuelle examine de nouveau le comportement en transition des pièces soudées en acier HSLA-65 dans le cadre d’essais dynamiques de résistance à l’arrachement, où les éprouvettes sont beaucoup plus grandes que dans les essais Charpy et qui permettent de prévoir avec plus de précision le comportement des structures de grande taille. L’étude actuelle porte également sur une autre méthode permettant de déterminer l’énergie absorbée durant un essai dynamique de résistance à l’arrachement, à l’aide de la définition intégrale du travail.

Les résultats de cette étude montrent que les températures de transition déterminées par les essais dynamiques de résistance à l’arrachement sont beaucoup plus élevées que celles déterminées par les essais Charpy. Pour chaque soudure, plusieurs zones ont été soumises à des essais. Dans tous les cas, la ligne de fusion de la soudure s’avère posséder la température de transition la plus élevée, et la zone affectée par la chaleur a la température de fusion la plus basse; quelque part entre les deux se trouve le métal soudé. Selon une exigence de température de transition inférieur à -40°C, aucune des soudures soumises aux essais ne s’est avérée apte au service dans des conditions arctiques.

Executive summary

Ductile to Brittle Transition Behaviour of HSLA-65 Steel Welds: Dynamic Tear Testing

Neil Aucoin; DRDC Atlantic TM 2010-220; Defence R&D Canada – Atlantic; January 2011.

Introduction or background: HSLA-65 (ASTM A945, grade 65) is being considered for use as a naval ship steel for future platforms. Because future platforms could see Arctic service conditions, a detailed knowledge of the mechanical properties of welded HSLA-65 steel at temperatures down to -40°C was required. The ductile to brittle transition behaviour was examined for five different welded plates. Several areas of the welds were examined, including the weld metal, the fusion line, and the heat affected zone. Transition behaviour results are compared to previously obtained transition curves determined through Charpy impact testing.

A secondary goal of this study was to compare the standard ASTM E604 method of measuring absorbed energy in a dynamic tear test to an alternate approach using the integral definition of work.

Results: The results of this study show that transition temperatures determined through dynamic tear testing are much higher than those determined through Charpy impact testing, supporting the requirement for both tests, as stated in the Canada National Defence Standard D-49-003-003/SF-001. In all cases, the fusion line of the weld was found to have the highest transition temperature, the heat affected zone was found to have the lowest transition temperature, and the weld metal fell somewhere in between.

Though the integral definition of work method was able to follow the transition trends as well as the standard conservation of energy approach, the two energy values did not agree. A difference between the two methods was found to increase approximately linearly with increasing absorbed energy, suggesting a systematic error was present in the method.

Significance: Based on a transition temperature requirement of less than -40°C, none of the welds tested were found to be fit for use on future platforms which could see service in Arctic conditions. The results show that Charpy impact testing is not a reliable method of determining transition behaviour of larger scale structures. Also, the results show that testing of only the weld metal, as recommended in the Canada National Defence Standard D-49-003-003/SF-001, may not be representative of a worst-case scenario, as the results of this study show that the fusion line of the weld is more susceptible to brittle fracture than the weld metal.

Future plans: More work is required to determine the cause of the difference between the two energy measurement methods used. Prime suspects are the calibration of the force sensor and the accuracy of the velocity and displacement measurement of the falling mass.

Sommaire

Ductile to Brittle Transition Behaviour of HSLA-65 Steel Welds: Dynamic Tear Testing

Neil Aucoin; DRDC Atlantic TM 2010-220; R et D pour la défense Canada – Atlantique; janvier 2011.

Introduction : L'utilisation de l'acier HSLA-65 (ASTM A945, nuance 65) est envisagée pour la construction de plateformes de bâtiment naval à venir. Comme les plateformes futures risquent d'être utilisées dans des conditions arctiques, une connaissance approfondie des propriétés mécaniques de l'acier HSLA-65 soudé jusqu'à -40°C est requise. Le comportement en transition ductile à fragile de cet acier a été examiné pour cinq plaques soudées différentes. Plusieurs zones des soudures ont été examinées, y compris le métal soudé, la ligne de fusion et la zone affectée par la chaleur. Les résultats des données sur le comportement de transition sont comparés aux courbes de transition obtenues antérieurement à l'aide de l'essai de choc Charpy.

Un objectif secondaire de la présente étude consistait à comparer la méthode indiquée dans la norme ASTM E604 visant à mesurer l'énergie absorbée dans un essai de résistance à l'arrachement à une autre méthode utilisant la définition intégrale du travail.

Résultats : Les résultats de la présente étude montrent que les températures de transition obtenues lors de l'essai dynamique de résistance à l'arrachement sont beaucoup plus élevées que celles obtenues à l'aide de l'essai de choc Charpy, ce qui appuie l'exigence pour les deux essais, tel qu'indiqué dans la norme D-49-003-003/SF-001 de la Défense nationale du Canada. Dans tous les cas, la ligne de fusion de la soudure s'est avérée l'endroit où la température de transition est la plus élevée, la zone affectée par la chaleur est l'endroit où la température de transition est la plus basse et la température se situe à peu près entre les deux pour ce qui est du métal d'apport.

Bien que la méthode de la définition intégrale du travail ait suivi les tendances de la transition ainsi que l'approche classique de la conservation d'énergie, les deux valeurs obtenues pour l'énergie ne concordait pas. Il existe une différence entre les deux méthodes qui augmente à peu près linéairement avec l'énergie absorbée, ce qui laisse entendre qu'une erreur systématique est présente dans la méthode.

Portée : Pour une température de transition inférieure à -40°C, aucun des essais sur les soudures n'a permis de déterminer que l'acier était apte à une utilisation sur de futures plateformes qui pourraient servir dans des conditions arctiques. Les résultats montrent que l'essai de choc Charpy ne constitue pas une méthode fiable permettant de déterminer le comportement de transition des structures à plus grande échelle. De plus, les résultats montrent que les essais portant uniquement sur le métal soudé, comme le recommande la norme D-49-003-003/SF-001 de la Défense nationale du Canada, pourraient ne pas être représentatifs du scénario du pire cas, car la ligne de fusion de la soudure est plus sujette à la rupture fragile que le métal soudé.

Perspectives : D'autres travaux sont requis pour déterminer la cause de la différence entre les deux méthodes de mesure employées. Les principaux aspects à étudier sont l'étalonnage du

capteur de force et l’exactitude de la mesure de la vitesse et du déplacement de la masse qui tombe.

This page intentionally left blank.

Table of contents

List of figures

List of tables

Acknowledgements

Dr. Christopher Bayley, DRDC Atlantic – Dockyard Laboratory Pacific, is acknowledged for providing valuable materials science information and advice.

This page intentionally left blank.

1 Introduction

This report summarizes the impact testing of five different welded joints constructed from ASTM A945/A945M grade 65 (HSLA-65) steel plate [1]. HSLA-65 plate is considered as a possible replacement to conventional shipyard high strength steels, as its higher yield strength and good weldability make it a good candidate for creating thinner, lighter structures. Bayley states that previous design studies of destroyer type hulls showed that the benefits of higher strength steels (i.e. 80 ksi yield strength) are limited by a buckling failure mode, and that HSLA-65 could be used to achieve structures of similar weight [2].

Before this steel can be used to build future surface platforms, which will likely be required to withstand arctic service conditions, a detailed knowledge of the low temperature toughness of the steel and its welds is required. This work completes the impact characterization of the welded connections reported by Bayley [2] and Pussegoda [3] examining the effects of heat input on fracture characteristics of HSLA-65.

The goals of these tests were to:

1. Evaluate the ductile to brittle transition temperature of the HSLA-65 welds using a drop tower.

2. Compare dynamic tear test results to previously recorded Charpy test results of the same welds.

3. Develop an expertise in dynamic tear testing and compare two methods of measuring the energy absorbed during a dynamic tear test.

4. Evaluate if the tested welded plates are fit for service at a design temperature of -40 °C.

5. Comment on the testing requirements of the D-49-003-003/SF-001 standard for welding HMC Ships and Auxiliaries [4].

One of the original goals of this testing was to evaluate the effects of using a closely matched weld metal (MIL-71T1-HYN, 70 ksi minimum yield) versus an overmatched weld metal (MIL-101TM, 100 ksi minimum yield) on the fracture properties of HSLA-65 steel FCAW welds. However, tensile testing performed in [2] revealed that the as-welded metals had very similar yield strengths of approximately 100 ksi (690 MPa), eliminating the possibility of a meaningful comparison.

2 HSLA-65 Welded Plates

Five different welded plates were fabricated using different weld consumables, weld procedures and heat inputs. Welded plates A, B, C, and D were joined using a flux core arc welding (FCAW) process, while plate G was joined using a gas metal arc welding (GMAW) process. All FCAW welds were performed on 15.8 mm (5/8") thick plate, while GMAW welds were performed on 9.5 mm (3/8") plate. The chemical compositions of the plates are listed in Table 1. GMAW welds used an AWS ER70S-6 consumable with a single heat input. Within the FCAW welded specimens, plates were welded with either high or low heat inputs with one of two consumables: MIL-71T1-HYN or MIL-101TM. All welds were performed using a 75%Ar, 25%CO_2 gas mixture.

The original experimental plan included a comparison of the toughness of a closely matched consumable (MIL-71T1-HYN, 70 ksi minimum yield strength) and an overmatched consumable (MIL-101TM, 100 ksi minimum yield strength). However, subsequent tensile tests revealed that the as-welded consumables had very similar yield strengths. High heat input welds resulted in four passes per plate, while low heat input corresponded to eight passes per plate. A summary of the welding procedures for each plate is listed in Table 2.

Table 1: Plate chemical compositions (wt%) [5]

Plate Thickness	Heat Number	C	Mn	P	S	Si	Cu	Ni	Cr
5/8 inch	822K30990	0.08	1.44	0.015	0.004	0.308	0.019	0.02	0.04
3/8 inch	833K60400	0.08	1.43	0.02	0.004	0.299	0.02	0.01	0.04

Continued:		Mo	V	Ti	Al	B	Nb	N
5/8 inch	822K30990	0.01	0.071	0.015	0.02	0.0002	0.034	0.006
3/8 inch	833K60400	0.006	0.067	0.016	0.03	0.0002	0.035	0.008

Table 2: Summary of welding procedures [2]

Plate	Welding Process	Consumable	Average Heat Input (kJ/mm)
A	FCAW	MIL-71T1-HYN	1.2
B	FCAW	MIL-71T1-HYN	2.2
C	FCAW	MIL-101TM	1.2
D	FCAW	MIL-101TM	2.3
G	GMAW	AWS ER70S-6	2.0

Dynamic tear specimens were machined with reference to ASTM E604 [6], and crack initiating notches were placed in several different locations: In the weld material (W), on the fusion line (F), and 1 mm outside the fusion line in the heat affected zone (F+1). The specimens notched on the fusion line were machined and tested after the testing of "W" and "F+1" type specimens were complete. It was decided that fusion line notched specimens of the high heat input welds (B and D) were not necessary as their fracture properties were already determined to be inferior to the

low heat input welds (A and C). A summary of the notch locations used with each specimen type is shown in Table 3. The three notch locations are illustrated in Figure 1.

Table 3: Specimen notch locations

Welded Plate Type	Drop Tower Specimens
A	F, W, F+1
B	W, F+1
C	F, W, F+1
D	W, F+1
G	W, F+1

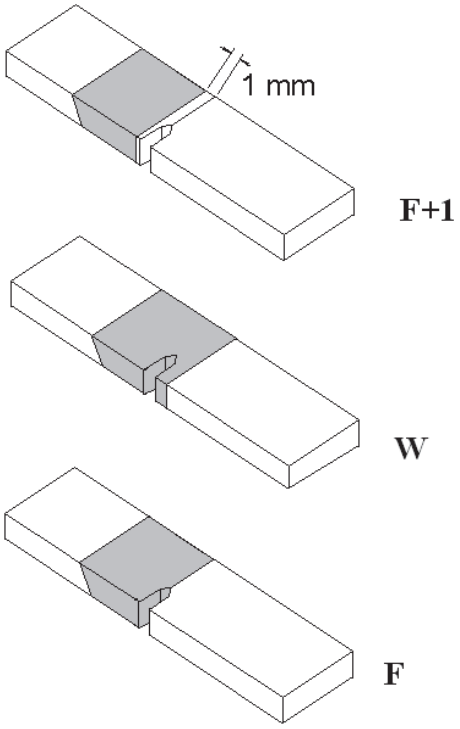

Figure 1: Specimen notch locations, where the grey area represents weld metal

2.1 Welding Defects

All "D" type welded plates had a slag inclusion in the root of the weld due to a repair pass during the welding procedure. Figure 2 shows a sectioned view of the "D" welded plate. The slag inclusion ran the entire length of the plate and is evident in all "D" specimens. A similar, though smaller, inclusion was found in several "B" welds.

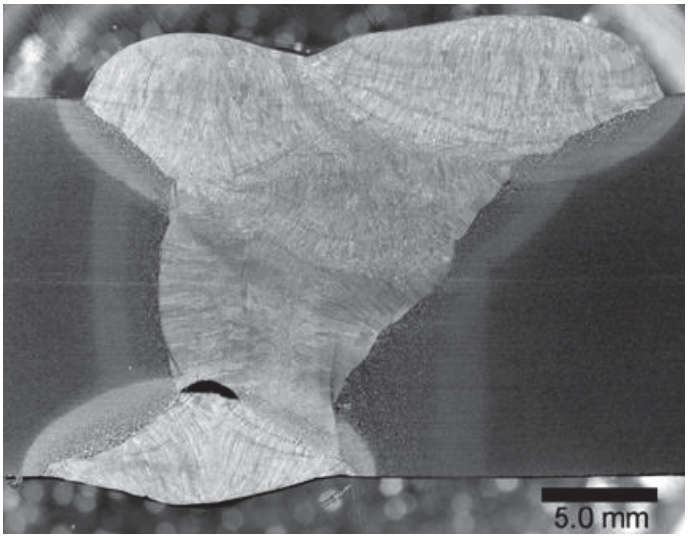

Figure 2: “D” welded plate slag inclusion

3 Drop Tower Impact Testing

3.1 Dynamic Tear Test Method

Impact testing of HSLA-65 welded specimens was performed with reference to the ASTM E604 standard [6]. The ASTM E604 dynamic tear test is a method of measuring the amount of energy absorbed by a test specimen during fracture when subjected to impact loading. The goals of impact testing were as follows:

- Develop an expertise in dynamic tear testing.
- Examine alternative methods of evaluating absorbed energy.
- Determine the ductile to brittle transition temperature for each welded plate based on absorbed energy and percent shear fracture surface area.

While most of the standard test procedure was followed, there were several notable differences, including:

- Specimens were 10 mm thick (FCAW welded plates) and 7.5 mm thick (GMAW welded plate) rather than the standard 16 mm thick.
- Impacts conducted at approximately 3.1 m/s, which is below the recommended minimum of 4 m/s.
- Frictional losses of drop tower were slightly greater than 1%.
- The profile of the striker tup was not fully semi-circular.

These differences prevent the reporting of valid ASTM E604 absorbed impact energies. It should be noted that these results may be representative only of material thicknesses of 10 mm and less. Thicker material tends to show transition behaviour at higher temperatures.

3.2 Drop Tower Configuration

Figure 3 shows a top down view of the drop tower. Drop tests were performed with a cross head mass of 362 kg free-falling from 50 cm. A close up of the test specimen, the anvils, and tup are shown in Figure 4. All sensors were connected to a National Instruments data acquisition system run through LabView. Data acquisition was set to trigger off a rising voltage from the optical sensor, and set to run for 0.1 seconds at a sampling rate of 100 kHz.

Figure 3: Top down view of the drop tower without specimen or anvils in place

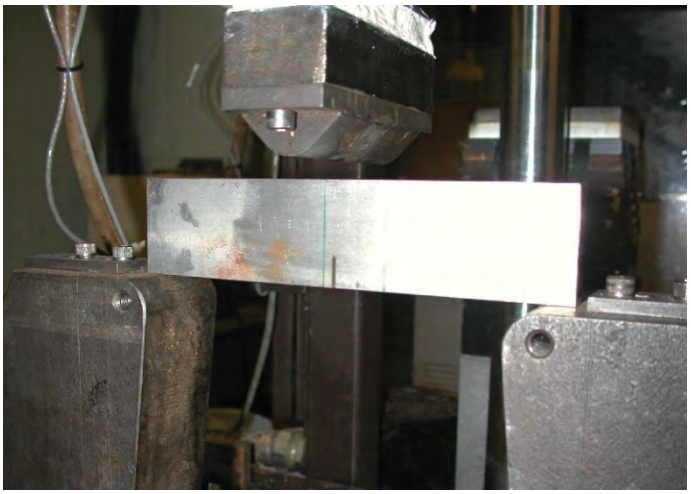

Figure 4: Drop tower anvil, specimen and tup

3.3 Energy Calculations

Two methods of calculating the absorbed energy were developed from the signal outputs recorded during the impact event. They differ in the approaches used to determine energy and are based on either the conservation of energy or the integral definition of work.

3.3.1 Conservation of Energy

The standardized dynamic tear test, defined in ASTM E604, is based on the conservation of energy. Measurements of height – h and velocity – v are made prior to impact and again shortly

after impact. The total energy (E_{Total}), Eq. (1), of the striker at any instant is the sum of the potential energy, Eq. (2), and kinetic energy, Eq.(3). The difference between the total energy before impact and the total energy after impact is the energy absorbed by the specimen during fracture, Eq.(4).

$$E_{Total} = E_{potential} + E_{kinetic} \tag{1}$$

$$E_{potential} = mgh \tag{2}$$

$$E_{kinetic} = \frac{1}{2}mv^2 \tag{3}$$

$$E_{absorbed} = m\left(g(h_{initial} - h_{final}) + \frac{1}{2}\left(v_{initial}^2 - v_{final}^2\right)\right) \tag{4}$$

E=energy, m=mass, g=gravitational acceleration, h=height, v=velocity

The standard approach is to calculate the velocity just prior to impact and after a minimum of 2 inches (50.8 mm) after impact. The current method took the second velocity measurement 55 mm after impact. An incremental absorbed energy is computed using Eq. (4) at each time step in the acquired data, which provides sufficient data to display the increment of energy absorbed as a function of tup travel. The velocity is determined using the frequency of the interrupted light beam signal and the known spacing of the interrupting flag. The arrangement of the light velocity system is shown in Figure 5 while a scan of the flag is shown in Figure 6. In the arrangement shown in Figure 5, the source light beam is interrupted by the black bars of the flag when it passes in between the source and sensor. The total displacement is determined by integrating the velocity data with respect to time. The post processing algorithm for the velocity flag is listed in Annex A.

A limitation with this approach is the accuracy of the velocity measurement, arising from finite inconsistencies in flag spacing (imperfectly spaced lines on the flag due to limited printing accuracy) and the flexibility of the printed sheet. These errors limit the velocity measurement accuracy.

Numerically, the absorbed energy can be determined from each time step as shown in Eq. (5).

$$E_A = \sum m\left(g\left(V_i - V_{i-1}\right)\Delta t\right) + \frac{1}{2}\left(V_{i-1}^2 - V_i^2\right) \tag{5}$$

where *i* denotes the current time step. The displacement term is opposite to that shown in Eq.(4) to show that increasing displacement corresponds to decreasing potential energy, due to the direction of the weight's velocity through impact (i.e. falling mass).

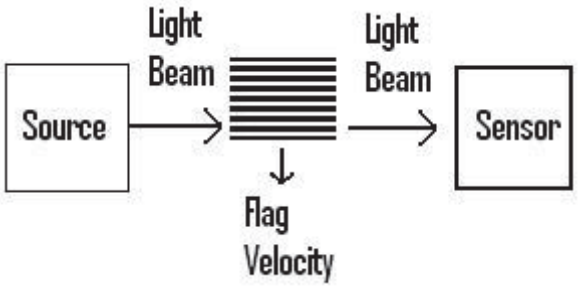

Figure 5: Optical velocity sensor operation

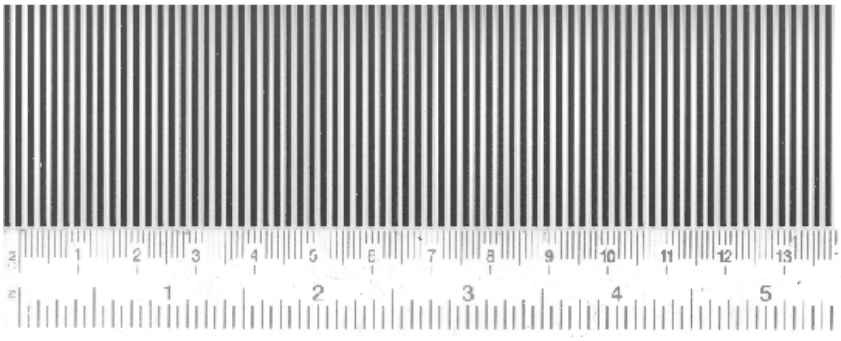

Figure 6: Optical flag

3.3.2 Integration of Force vs. Displacement Data

A second method of measuring the energy absorbed by each specimen was investigated, based on the integral definition of work, defined by Eq. (6), in which a force *F* is integrated over a distance *x*. This integral was calculated numerically using a trapezoidal approximation of the force displacement record.

$$W = \int_{x_1}^{x_2} F(x)dx \tag{6}$$

The advantage of this energy formulation is that it integrates the force and displacement outputs, which are potentially more repeatable than the current velocity output, as the velocity is integrated to obtain displacement, which tends to smooth the data. Though, this second method was investigated, the energies used to examine the ductile-brittle transition temperatures are based on the ASTM E604 recommended approach of conservation of energy.

3.4 Dynamic Tear Test Specimen Preparation

3.4.1 Specimen Machining

Dynamic tear specimens from welded plates A, B, C, and D were machined according to ASTM E604, as shown in Figure 7, with the exception of the thickness, B. Specimens from plate G (GMAW weld) had a thickness of 7.5 mm, while all other specimens had a thickness of 10 mm. The notch locations for each specimen are listed in Table 3.

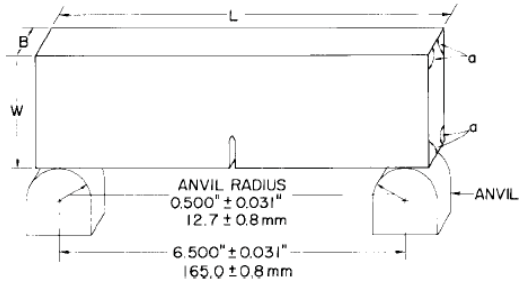

Dimensions and Tolerance for Specimen Blank

Parameter	Units	Dimension	Tolerance
Length, *L*	in.	7.125	±0.125
	mm	181	±3
Width, *W*	in.	1.60	±0.10
	mm	41	±2
Thickness, *B*	in.	0.625	±0.035
	mm	16	±1
Angularity, α	deg	90	±1

Figure 7: Dynamic tear specimen dimension requirements [6]

3.4.2 Knife Edge Pressing

Prior to dynamic tear testing, the tip of each machined notch was sharpened by pressing a hard (60 Rockwell C) knife edge blade into the notch tip. This sharpened notch reduces the energy required for crack initiation and improves the repeatability of the fracture path. The dimensions of the sharpened pressed notch tip are shown in Figure 8. Measured pressed notch dimensions can be found in Annex B.

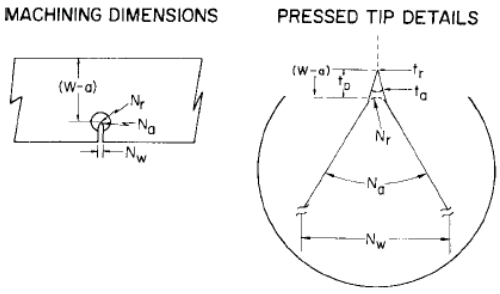

Dimensions and Tolerances for Notch Tip

Parameter	Units	Dimension	Tolerance
Net width, $(W - a)$	in.	1.125	±0.020
	mm	28.6	±0.5
Machined notch width, N_w	in.	0.0625	±0.005
	mm	1.59	±0.13
Machined notch root angle, N_a	deg	60	±2
Machined notch root radius, N_r	in.	0.005	max
	mm	0.13	max
Pressed tip depth, t_D	in.	0.010	±0.005
	mm	0.25	±0.13
Pressed tip angle, t_a	deg	40	±5
Pressed tip root radius, t_r	in.	0.001	max
	mm	0.025	max

Figure 8: Sharpened notch tip dimensions [6]

The notches were pressed using a servo-hydraulic test frame. Steel shim stock was used to ensure that the knife edge blade was centered and oriented correctly in the machined notch. The notch pressing procedure was as follows:

- Apply preload of 100 N under force control.
- Zero actuator displacement.
- Move actuator 0.4 mm so that the knife edge is pressed into the notch tip.
- Unload specimen and optically measure the dimensions of the pressed notch tip.

3.4.3 Specimen Temperature Control

For tests other than those at room temperature, the specimens were soaked in a temperature controlled ethanol bath then quickly transferred to the drop tower. Specimens were left soaking for a minimum of 20 minutes prior to testing. All specimens were broken within 15 seconds of being removed from the bath. When the time to transfer the specimens took longer than 10 seconds, the fracture temperature was corrected from a series of temperature vs. time curves.

These surface temperature versus time curves were constructed for various temperatures using a thermocouple magnetically attached close to the notch. Because of the position of the thermocouple on the surface of the specimen, the resulting curves are a worst-case scenario for temperature change while out of the bath. The temperature vs. time curves for three bath temperatures are shown in Figure 9. The initial steady surface temperature shown in each curve is a convenient side effect of the ethanol evaporating off the surface of the specimen. From these curves, it can be seen that the surface temperature can change as much as 2°C over 15 seconds of

being out of the bath. This small change in temperature on the surface of the specimen is not expected to significantly affect the through thickness temperature of the specimen.

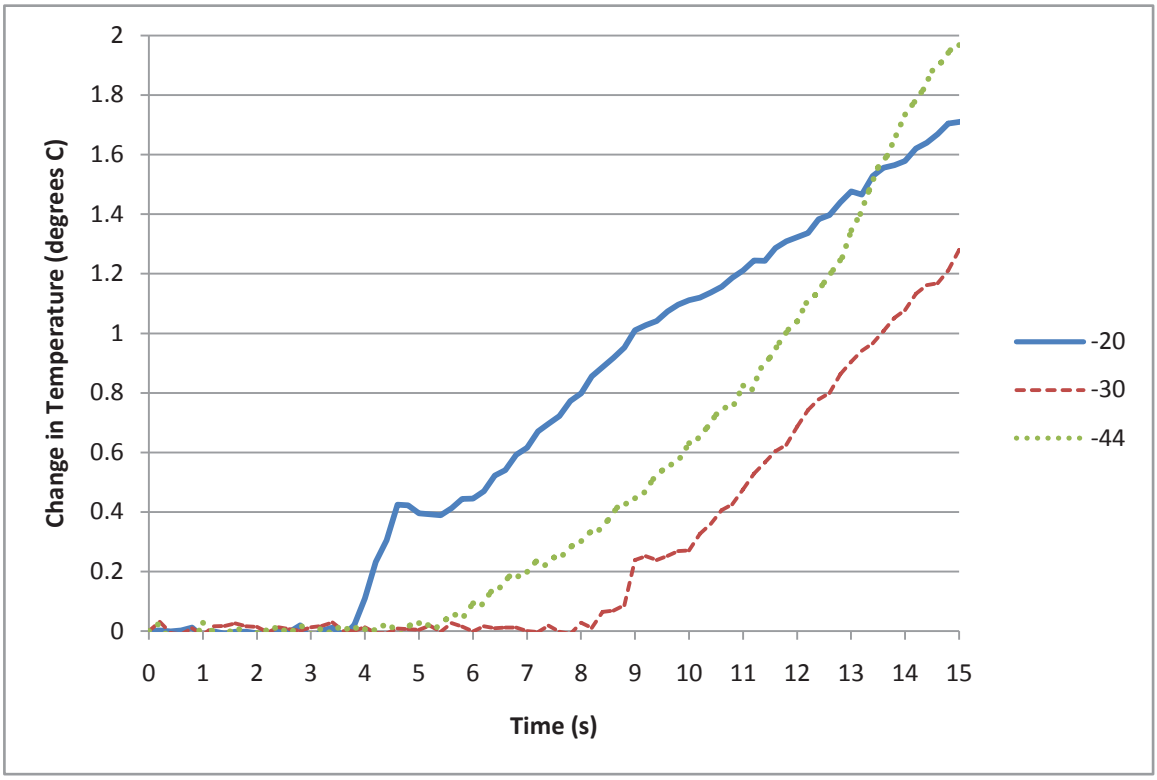

Figure 9: Change in specimen surface temperature vs. time curves

4 Results

For each welded plate, the transition from ductile to brittle fracture was evaluated based on the conservation of energy along with the percent shear fracture surface area. Due to problems encountered with the optical sensor some absorbed energy measurements are missing for some specimen/temperature combinations, with the full data set summarized in Annex C.

Two sets of sample data are shown in Figures 10 and 11 for a ductile and brittle fracture, respectively. These plots comprise of four quadrants, the upper two displaying the raw data of velocity and force versus time, while the bottom quadrants display the force and energy as a function of tup travel distance, such that impact occurs at 0 mm. In the force plots two peaks are clearly distinguished with first caused by the tup impacting the specimen and the second caused by the tup flanges contacting the specimen. This secondary impact is illustrated in Figure 12 and results from a non-semi-circular tup profile. Marks from this secondary impact are evident on the upper surface of all specimens where it was apparent on the specimens force graphs. However, as the absorbed energy is measured after a displacement of 55 mm this secondary peak was not included in the absorbed energies. The bottom right quadrant of the plots compares the two methods of determining the absorbed energy, in which the integral approach consistently under-predicts the absorbed energy.

The significant differences between the ductile and brittle modes of failure are visible in the velocity and force profiles. For a ductile fracture, the energy absorption results in a significant reduction in the tup velocity while a brittle fracture has only a small reduction in velocity. A complimentary trend can be seen on each force plot, where the peak force in a ductile fracture remains higher over a longer period of time compared to a brittle fracture.

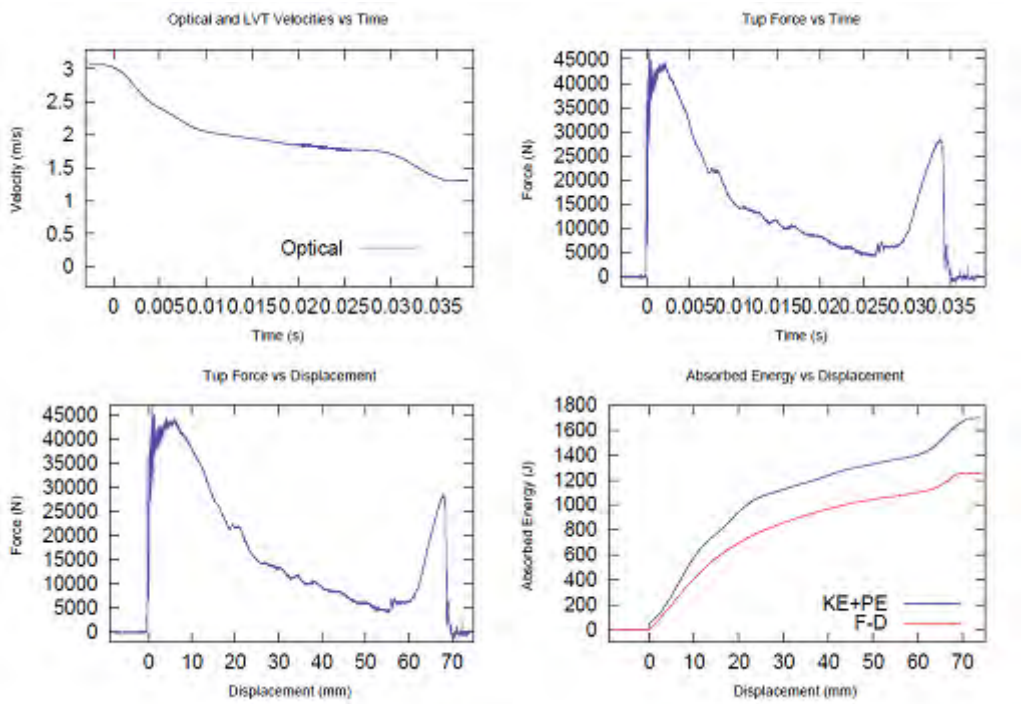

Figure 10: Fusion line notched specimen (A42) – ductile fracture tested at -10 °C

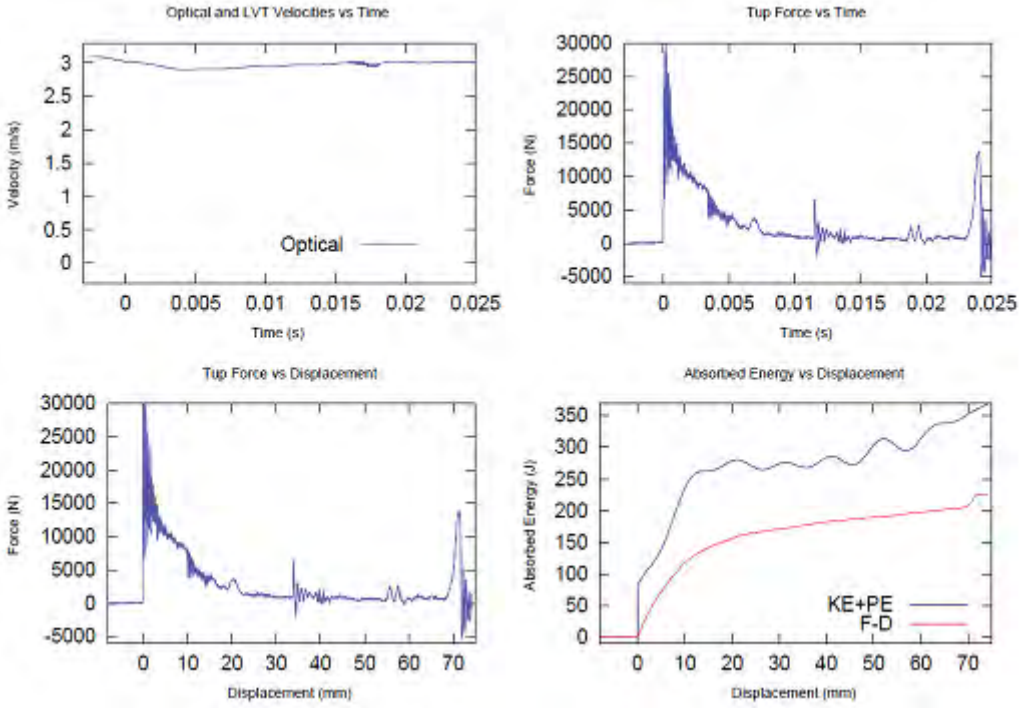

Figure 11: Fusion line notched specimen (A41) – brittle fracture tested at -40 °C

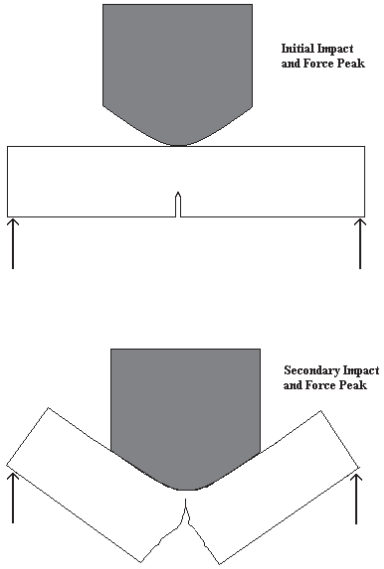

Figure 12: Cause of initial and secondary force peaks in dynamic tear test results

The measured ductile fracture surface area was assessed from the difference of the brittle area and total areas divided by the total area, as shown in Eq. (7), This procedure was easier to estimate the ductile fracture surface since the brittle area was generally more rectangular and thus, easier to measure. An example of fracture surface measurement is shown in Figure 13.

$$\%Ductile = \frac{A_{total} - A_{brittle}}{A_{total}} \times 100\% \tag{7}$$

Matthews [7] suggests that shear lip size is an effective alternate way of determining transition behaviour. However, many mixed mode fracture surfaces, such as shown in Figure 13, were observed due to the fracture path passing through several zones of the weld, as can be seen from a cross section of the weld in Figure 2. On these mixed mode surfaces, a measurement of maximum shear lip, as suggested in [7], would bias the results toward a lower transition temperature.

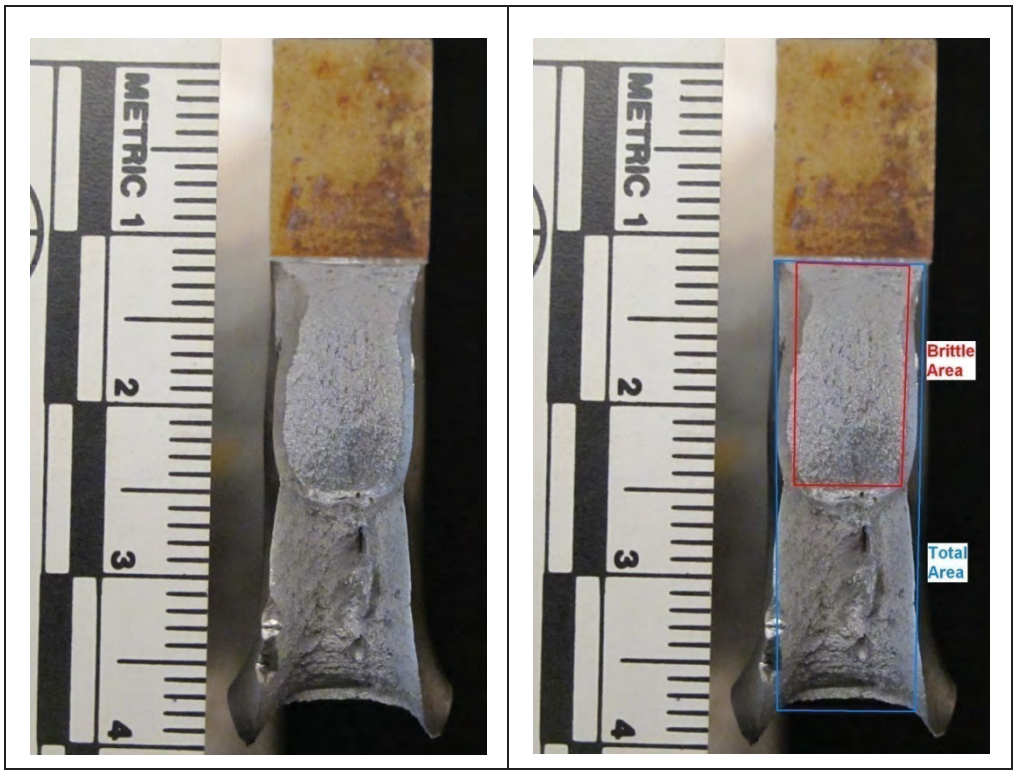

Figure 13: Example of a mixed mode fracture surface and the fracture surface area measurement method. The specimen was notched on the fusion line.

Absorbed energy vs. temperature and fracture surface appearance vs. temperature graphs for each type of welded plate is shown in Figure 10 through Figure 33. These graphs illustrate the following:

- Relatively high absorbed energies above the transition temperature range (upper shelf behaviour).
- High percentages of shear (ductile) fracture surface above the transition temperature range.
- Relatively low absorbed energies below the transition temperature range (lower shelf behaviour).
- Low percentages of shear (ductile) fracture surface below the transition temperature range.
- A good correlation exists between transition temperature ranges determined from measured absorbed energy, and from fracture surface appearance, as shown in Figure 14 through Figure 33.

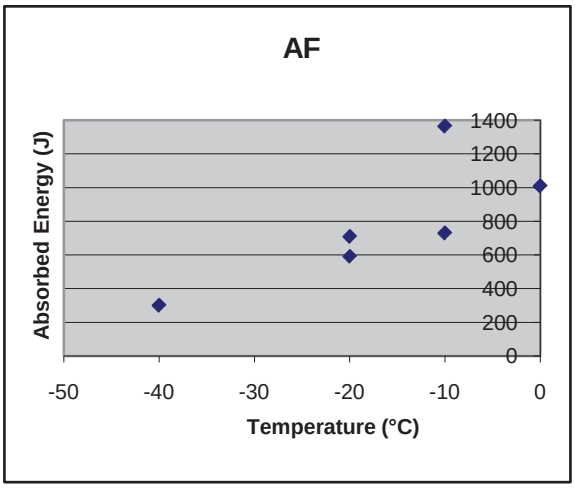

Figure 14: Weld panel A fusion line absorbed energy vs. temperature

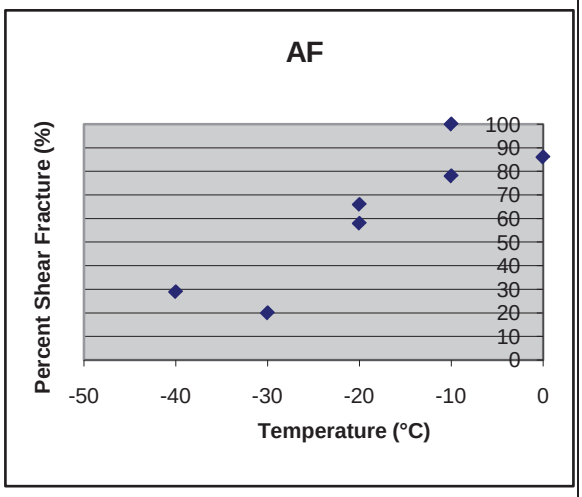

Figure 15: Weld panel A fusion line percent shear fracture vs. temperature

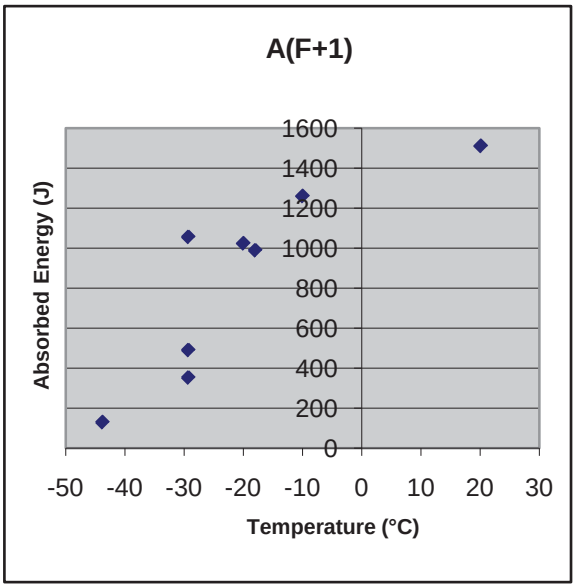

Figure 16: Weld panel A fusion line +1 mm absorbed energy vs. temperature

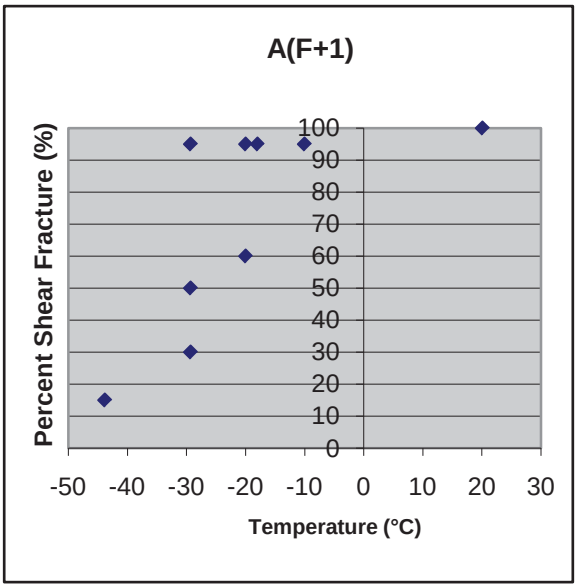

Figure 17: Weld panel A fusion line +1 mm percent shear fracture vs. temperature

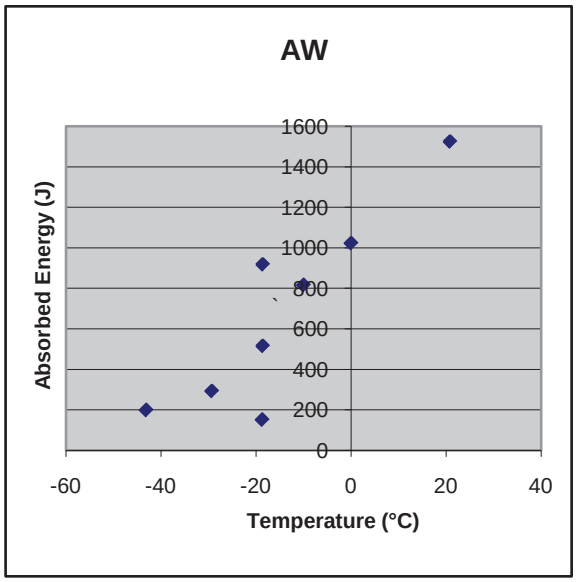

Figure 18: Weld panel A weld metal absorbed energy vs. temperature

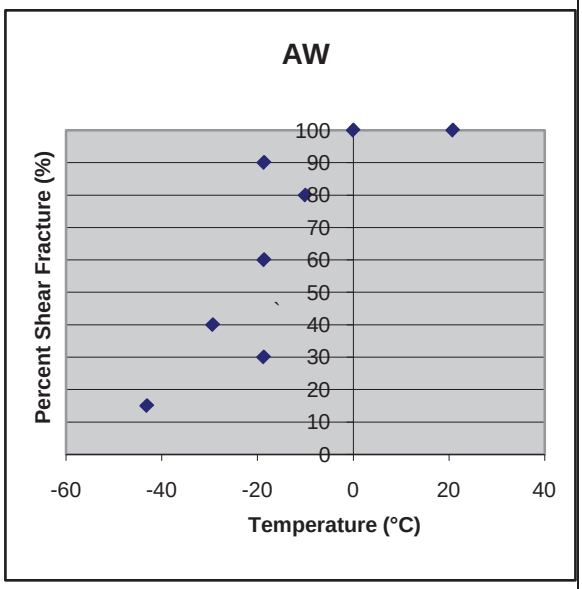

Figure 19: Weld panel A weld metal percent shear fracture vs. temperature

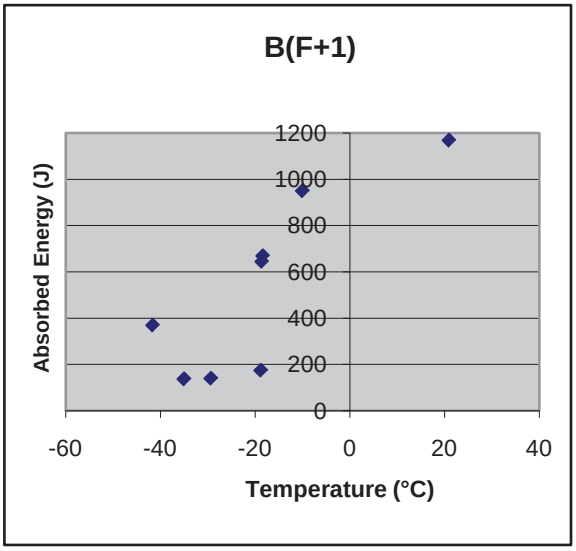

Figure 20: Weld panel B fusion line +1 mm absorbed energy vs. temperature

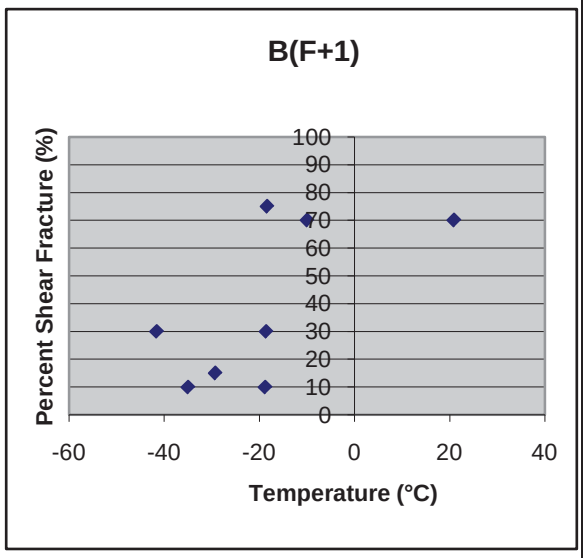

Figure 21: Weld panel B fusion line +1 mm percent shear fracture vs. temperature

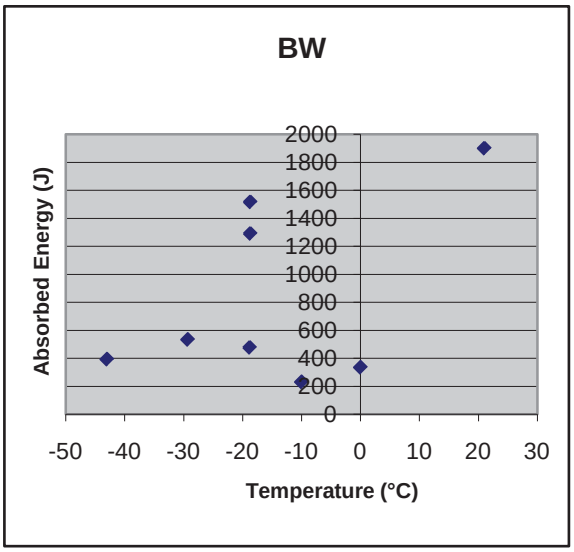

Figure 22: Weld panel B weld metal absorbed energy vs. temperature

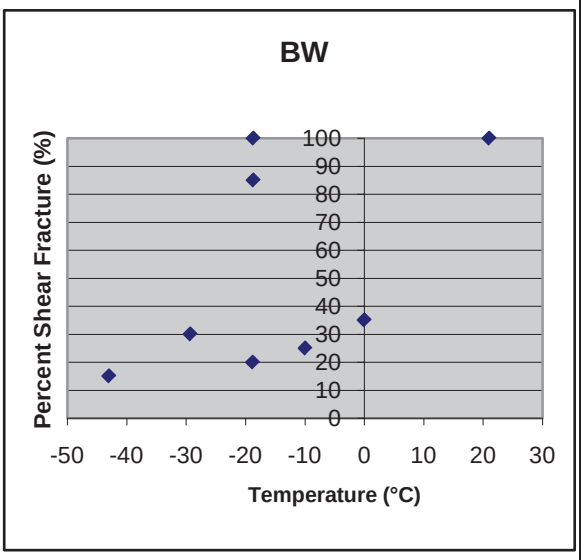

Figure 23: Weld panel B weld metal percent shear fracture vs. temperature

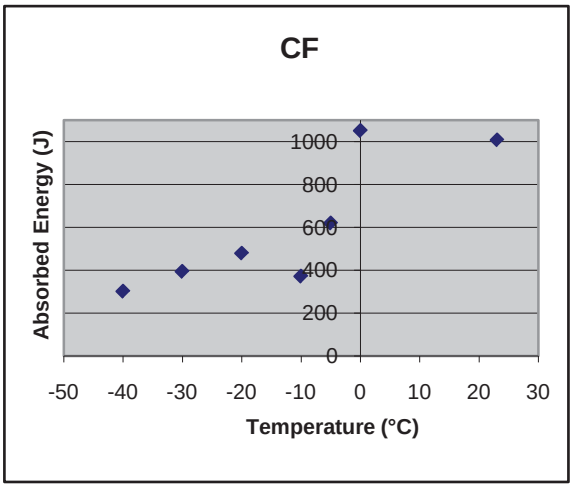

Figure 24: Weld panel C fusion line absorbed energy vs. temperature

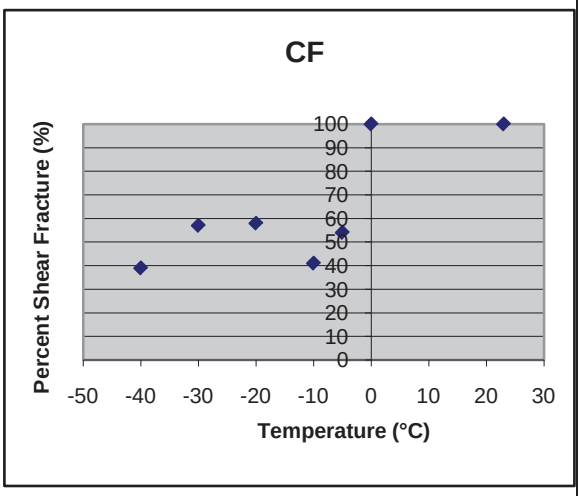

Figure 25: Weld panel C fusion line percent shear fracture vs. temperature

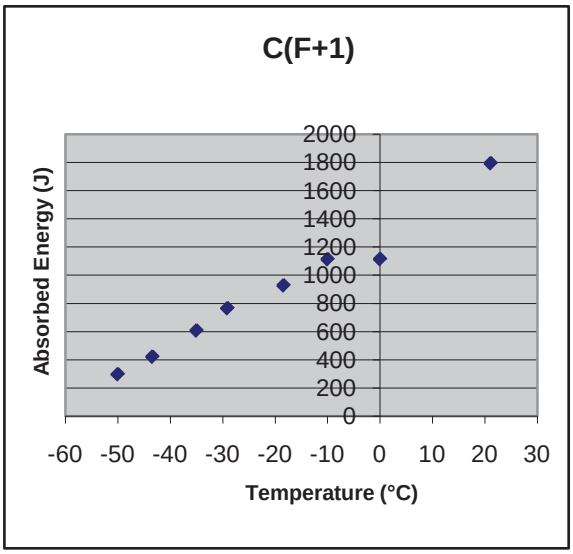

Figure 26: Weld panel C fusion line +1 mm absorbed energy vs. temperature

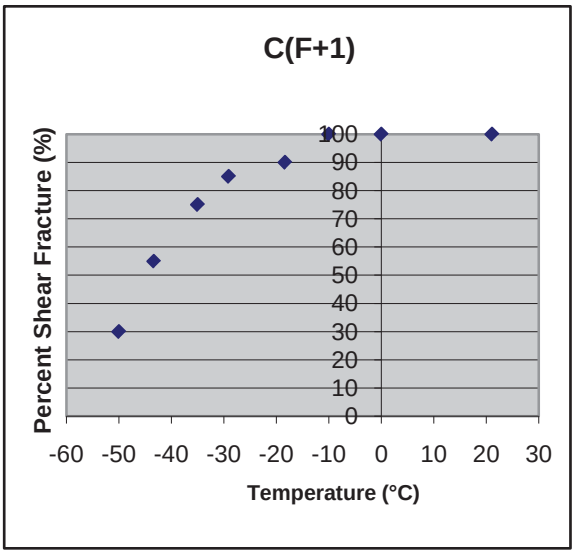

Figure 27: Weld panel C fusion line +1 mm percent shear fracture vs. temperature

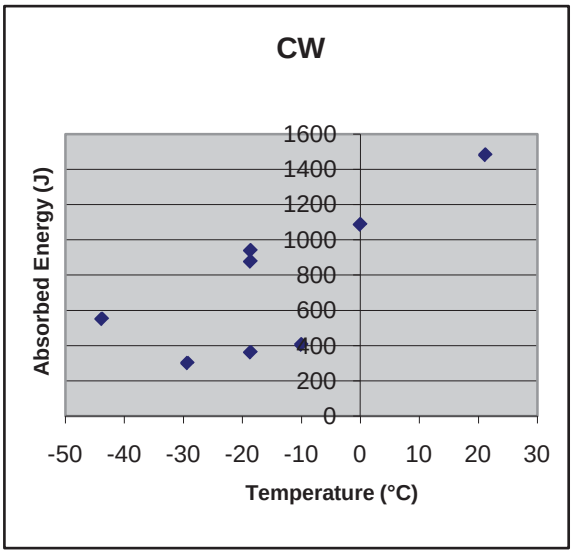

Figure 28: Weld panel C weld metal absorbed energy vs. temperature

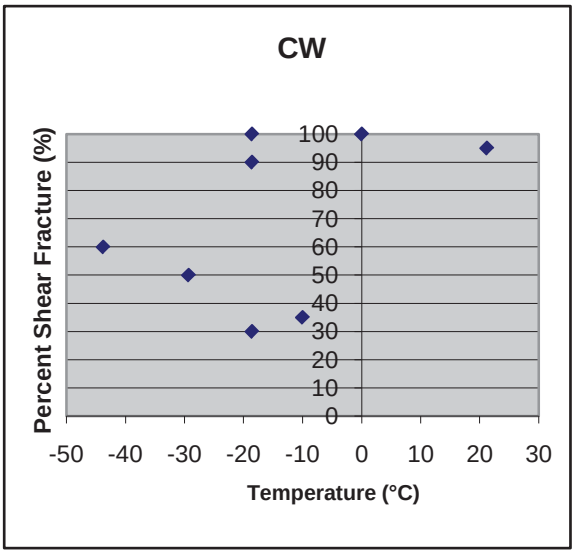

Figure 29: Weld panel C weld metal percent shear fracture vs. temperature

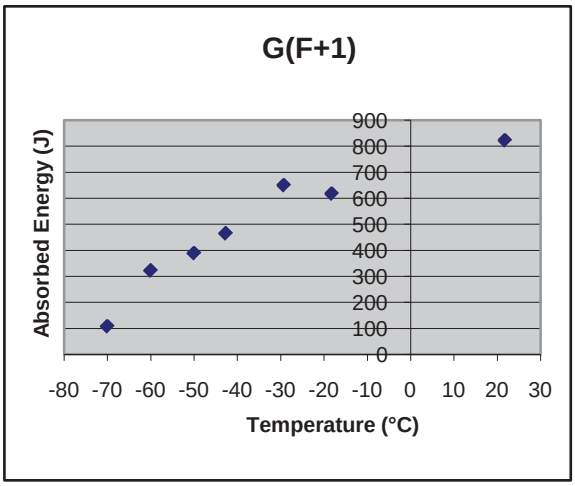

Figure 30: Weld panel G fusion line +1 mm absorbed energy vs. temperature

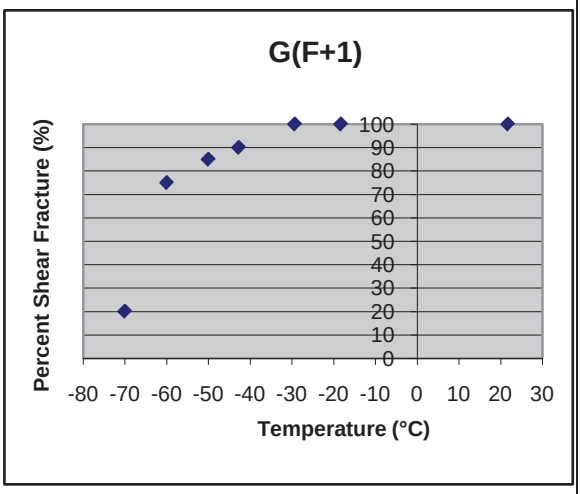

Figure 31: Weld panel G fusion line +1 mm percent shear fracture vs. temperature

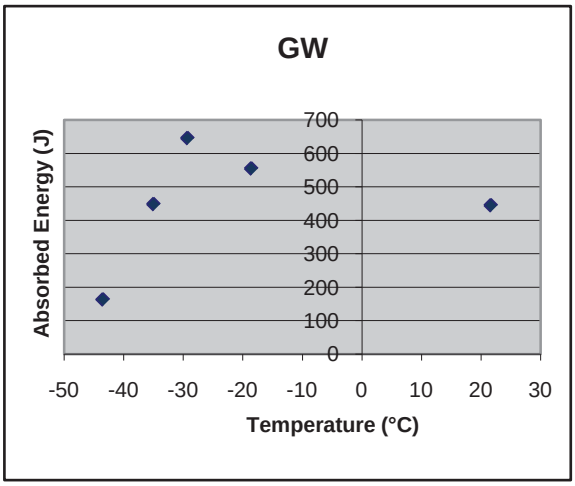

Figure 32: Weld panel G weld metal absorbed energy vs. temperature

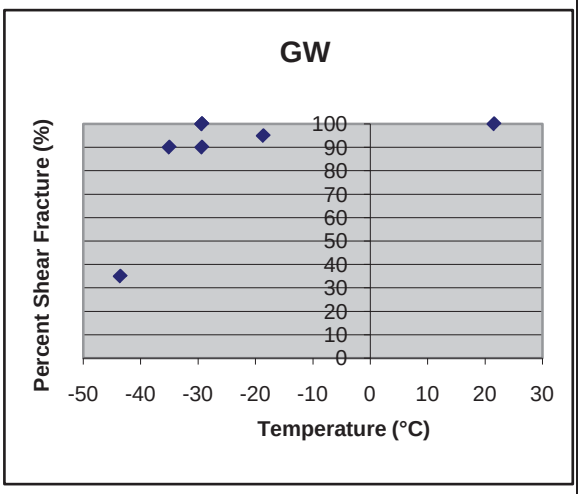

Figure 33: Weld panel G weld metal percent shear fracture vs. temperature

4.1 Discussion of Dynamic Tear Test Results

4.1.1 Comparison of Energy Measurement Methods

The absorbed energy determined from the integration of force vs. displacement data was consistently less than the absorbed energy determined from the change in kinetic and potential energy. Data comparing the two energy measurement methods is summarized in Annex C.1, and plotted in Figure 34, from which the following observations are made:

- The absolute difference in energies increases approximately linearly with absorbed energy, which suggests a systematic error in either the data acquisition or post-processing.

- Percent differences vary the least between the two energy measurement methods for mid to high absorbed energy ranges.

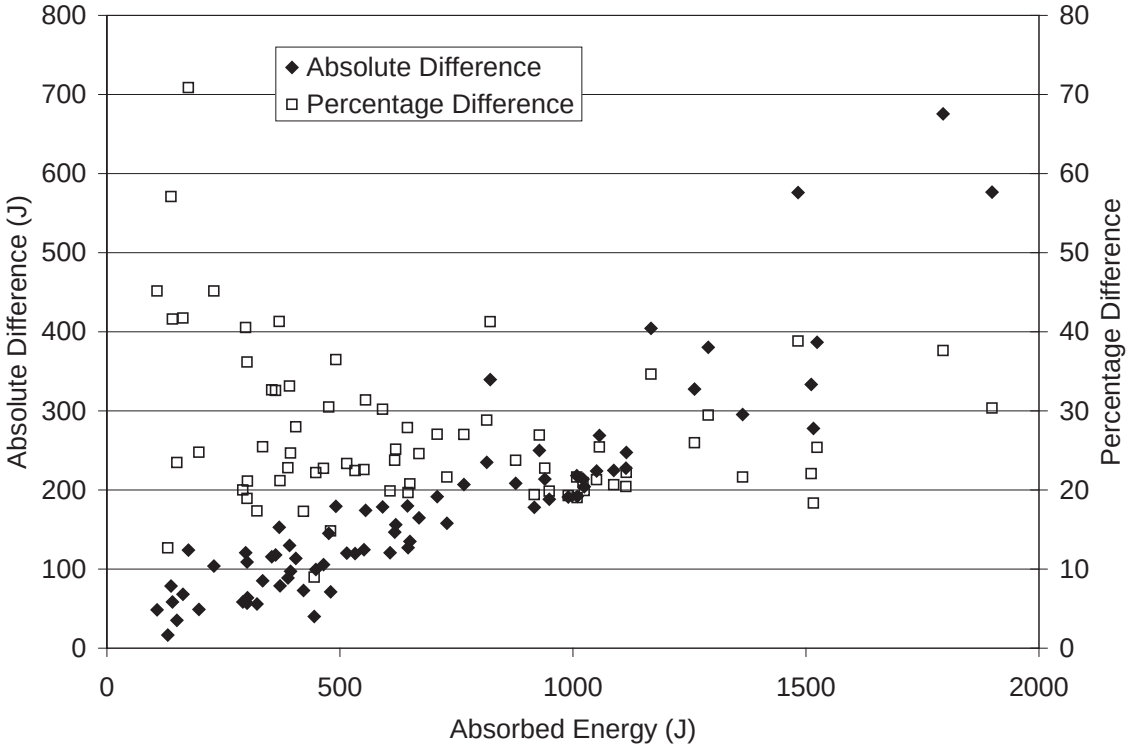

Figure 34: Comparison of absolute and percentage differences between the two calculation approaches.

Possible causes of the difference between the two energy measurement methods are listed in Table 4.

Table 4: Potential factors accounting for the difference in absorbed energy

Factor	Effects on Energy Method	Effects on Force Integration
Light sensor or flag inaccuracy	Affects velocity and displacement	Only affects displacement
Force calibration errors	No effect	Any errors in calibration directly affect absorbed energy
Quasi-static force sensor calibration	No effect	Possible dynamic effects not accounted for
Mass measurement of drop weight and tup	measured energy is directly proportional to mass	No direct effect

Based on this potential error analysis, the most likely causes are accuracy of the drop weight and tup mass, calibration of the dynamic force tup, and the accuracy of the velocity measurement.

4.1.2 Discussion of Specimen Transition Temperature

Dynamic tear test results are shown in Annex C. From this data, a summary of transition temperature ranges was created for each specimen type, shown in Table 5. Transition temperatures were determined as follows:

- Determine the mid-shelf energy as the average of the maximum upper shelf energy and the minimum lower shelf energy.
- Locate adjacent points above and below this mid-shelf energy level (highest temperature pair only in the case of scattered data in this region).
- Linearly interpolate between these points to the previously determined mid-shelf energy.
- Determine the corresponding temperature and round to the nearest 5 °C.

The design intent is to use this steel for welded structures which will see temperatures down to -40°C. Good design practice dictates the use of steel and welds with a transition temperature that is below the minimum design temperature in an attempt to avoid the possibility of unpredictable brittle fracture in all parts of the welded structure.

It can be seen that notch location significantly affects the transition temperature range of each weld type. Specimens notched 1 mm outside the fusion line in the heat affected zone tended to have the lowest (most desirable) transition temperature ranges. Specimens notched on the fusion line had the highest (least desirable) transition temperature range. None of the tested plates

exhibited fracture properties appropriate for service at temperatures of -40°C at all notch locations.

Though not all "D" type specimens were tested due to the large slag inclusion running through all specimens, shown in Figure 2, it is interesting to note that the few which were tested all exhibited fully brittle (low energy) fracture at room temperature. This illustrates the importance of good welding practices and thorough inspection of welds in order to avoid welding defects such as slag inclusions.

Specimen type "G" exhibited the best impact fracture properties. However, in addition to temperature, specimen size also affects the fracture properties of a material due to different stress distributions and constraints which are evident in different specimen thicknesses. Smaller or thinner specimens tend to be more likely to fracture in a ductile manner [8]. The similarity in chemical composition between the two plates, as shown in [5], suggests that the difference in fracture properties is not caused by the chemistry of the steel. The difference in fracture properties was either caused by the different welding procedure used (GMAW vs FCAW), or the thinner specimen geometry, or by a combination of the two.

Table 5: Transition temperature for HSLA-65 impact specimens

Specimen	Transition Temperature From Absorbed Energy (°C)	Transition Temperature From Fracture Surface Area (°C)	Transition Temperature from Charpy Results (°C) [2]
AF	-5	-20	n/a
A(F+1)	-25	-20	-50
AW	-10	-20	-45
B(F+1)	-20	-15	0
BW	10	10	-50
CF	-5	-5	n/a
C(F+1)	-15	-40	-50
CW	-5	-5	-40
D(F+1)	Above room temperature with slag inclusion	Above room temperature with slag inclusion	-5
DW	Above room temperature with slag inclusion	Above room temperature with slag inclusion	-40
G(F+1)	-40	-65	-40
GW	-35	-40	-30

Previous work was performed to determine the transition temperature of the five specimen types using Charpy v-notch specimens [2]. This previous Charpy testing predicted transition temperatures for all low heat input FCAW plates (Specimen types A and C) ranging from -40°C to -50°C, and transition temperatures for GMAW plates of approximately -30°C.

Drop tower dynamic tear testing shows that the Charpy tests, performed in [2], predict transition behaviour at a temperature below that of a larger specimen, as shown in Table 5. It can be

expected that the behaviour of the drop tower dynamic tear specimens approximates a ship's hull plate better than a Charpy specimen due to the larger size.

For all welded plates, it was found that specimens notched in the weld metal had the highest transition temperature range (least desirable situation) and specimens notched 1 mm outside the fusion line had the lowest transition temperature range (most desirable situation). After completing all "W" and "F+1" specimens, additional specimens were cut from welded plates A and C and notched on the fusion line of the weld. All fusion line notched specimens performed the worst out of the three notch locations.

Table 6: Test specimen quality trends

Most Desirable Properties
Lowest Transition Temperature Range
G(F+1)
GW
A(F+1)
B(F+1)
C(F+1)
AW
AF
CW
CF
BW
DW
D(F+1)
Highest Transition Temperature Range
Least Desirable Properties

Table 6 shows that both GMAW specimens displayed the lowest transition temperature. However, it is not known if this is because of a superior welding procedure, or due to the smaller specimen size used. For the FCAW welds, plates A and C (low heat input welds) displayed more desirable transition behaviour than plates B and D (high heat input).

The Canada National Defence standard D-49-003-003/SF-001 [4] requires one set of three dynamic tear specimens to be extracted and notched within the weld metal and tested at -29 °C. Though knowing the toughness of the weld metal is important, the weld metal may not be the most critical location in a welded structure. The results shown above indicate that, at least for the welds tested, the fusion line will show brittle behaviour at a higher temperature than the weld metal.

5 Conclusions and Recommendations

Of the three notch locations tested, specimens notched on the weld fusion line displayed the least desirable transition temperature range of the three notch locations. This behaviour was seen in both plates A and C, which were the only two plates where the fusion line was tested. For critical structures, four key locations should be tested for toughness when initially qualifying the material and welding procedure for use: base metal, weld fusion line, weld metal, and heat affected zone.

It can be seen from the dynamic tear test results and the Charpy impact results from [2], summarized in Table 5, that Charpy impact testing is not sufficient to determine the transition behaviour of a material. Larger scale test results, such as those from dynamic tear testing, offer a more reliable representation of the behaviour of structural size material, even when the specimen thickness is the same. However, based on the same reasoning, the results stated in this report may not be a reliable representation for welded structures which are thicker than 7.5 mm (GMAW welds) or 10 mm (FCAW welds).

Canadian National Defence Standard D-49-003-003/SF-001 [4] recommends impact testing of the weld metal only. The results of this report show that specimens notched on the fusion line will display brittle behaviour at a higher temperature than specimens notched in the weld metal. It is recommended that, for weld procedure qualification, both the weld metal and fusion line be tested for toughness using a dynamic tear test.

Some problems still exist with the current drop tower setup, where absorbed energies calculated from conservation of energy and integration of force versus displacement data do not agree. Future work is necessary to remedy this problem and increase confidence in drop tower results. A run of tests of the current system with a higher drop height is necessary before any changes to the current system are made.

References

[1] ASTM International. *Designation A 945/A945M – 95. Annual Book of ASTM Standards*, Volume 01.04. 2000 Ed.

[2] Christopher Bayley, Adam Mantei. *The Influence of Heat Input on the Fracture and Metallurgical Properties of HSLA-65 Steel Welds*. Defence R&D Canada – Atlantic. Technical Memorandum. DRDC Atlantic TM 2008-130, July 2008.

[3] Nick Pussegoda. *Fracture Toughness Characterization of HSLA Steel Weldments.* BMT Fleet Technology Limited. DRDC Atlantic CR-2008-114. 2003.

[4] Canada National Defence Standard. *D-49-003-003/SF-001. Welding Specification for HMC Ships and Auxiliaries*. 2003-05-01.

[5] ISG Burns Harbor Plate, Inc. *Quality Assurance Report of Tests and Analyses*. ASTM A945 grade 65 plates, heats 833K60400 and 822K30990. April 18, 2006.

[6] ASTM International. *Designation: E604-83 (Reapproved 2002). Standard Test Method for Dynamic Tear Testing of Metallic Materials.* Annual Book of ASTM Standards, Volume 03.01. 2008 Ed.

[7] J.R. Matthews, C.V. Hyatt, J.F. Porter, K.J. KarisAllen. *Effect of Thickness on the Relationship Between Shear Lip and Energy in Dynamic Tear Specimens*. Engineering Fracture Mechanics. Volume 60, Issue 5-6, Pages 529-542. 1998.

[8] D. J. Wulpi. *Understanding How Components Fail*. American Society for Metals (ASM) publication. 1985.

Annex A   Optical Velocity Post-Processing Algorithm

```
%%%%%%%%%%%%%%%%%%%%%%%%%%%%%%%%%%%%%%%%%%%%%%%%%%%%%%%%%%%%%%%%%%%%%%%%
%%%%%%%%%%%%%%%%%%%%%%%%%
%Author:    Neil Aucoin
%Date:            October 21, 2008
%
%Description:     Takes nx2 Data matrix from optical velocity
measurement (positive square wave)
%                 and determines the OPTICAL_PERIOD of the signal by
offsetting the data by the
%                 data's MEAN value to produce positive and negative
values, then finding
%                 the zero crossover points.  This is used to determine
the resulting velocity
%                 based on the known spacing of the clear and dark
sections of the
%                 optical sensor flags.
%
%Notes:           This program requires the clear and dark spacings on
the optical flag to be the same length in order to maximize
%                 output spatial resolution.
%                 Optical Velocity is speed only.  Direction cannot be
determined from this program.
%                 Optical velocity voltage output must be in column 2 of
Data matrix
%%%%%%%%%%%%%%%%%%%%%%%%%%%%%%%%%%%%%%%%%%%%%%%%%%%%%%%%%%%%%%%%%%%%%%%%
%%%%%%%%%%%%%%%%%%%%%%%%%
function INTERPOLATED_OPTICAL_VELOCITY = OpticalVelocity(DATA)

%measured optical sensor flag spacing (in meters)
SPACING=0.000997869;

%number of data points in Data matrix
n=length(DATA);

%Optical sensor gives about 6V when path is clear, and ~2V when path is
blocked.
MEAN=(max(DATA(:,2))+min(DATA(:,2)))/2

%offset Data to positive and negative values to simplify finding zeros
OFFSET_DATA=DATA;
for i=1:n
      OFFSET_DATA(i,2)=DATA(i,2)-MEAN;
end

%initialize variables and matrices
CROSS_TIME=[];
OPTICAL_PERIOD=[];
TEMP=[];
OPTICAL_VELOCITY=[];
j=1;
```

```
%find zero crossovers to determine period of signal
%zero crossovers = CROSS_TIME and are defined as the last point before
the crossover occurs
for i=1:n-1

      %zero crossover from negative to positive
      if (OFFSET_DATA(i,2)<=0 & OFFSET_DATA(i+1,2)>0)
            CROSS_TIME(j,1)=OFFSET_DATA(i,1);
            j=j+1;
      end

      %zero crossover from positive to negative
      if (OFFSET_DATA(i,2)>=0 & OFFSET_DATA(i+1,2)<0)
            CROSS_TIME(j,1)=OFFSET_DATA(i,1);
            j=j+1;
      end
end

%returns error if no optical velocity can be calculated from the Useful
Data set
if(length(CROSS_TIME) < 2)
      error('Unable to calculate a fringe crossing time from the Useful
Data set.  Check size of Useful Data set')
end

%number of rows in CROSS_TIME matrix
m=length(CROSS_TIME);

%determine the OPTICAL_PERIOD of zero crossover
for i=1:m-1
      OPTICAL_PERIOD(i,1)=CROSS_TIME(i+1,1)-CROSS_TIME(i,1);
end

%number of rows in OPTICAL_PERIOD matrix
o=length(OPTICAL_PERIOD);

%calculate optical velocity (in meters/second) based on frequency of
fringe
%crossing and physical spacing of fringes
for i=1:o
      OPTICAL_VELOCITY(i,1)=CROSS_TIME(i,1);
      OPTICAL_VELOCITY(i,2)=(1/OPTICAL_PERIOD(i,1))*SPACING;
end

%eliminate first and last optical velocity points, which appear to be
inaccurate and inconsistent
OPTICAL_VELOCITY=OPTICAL_VELOCITY(2:(length(OPTICAL_VELOCITY)-1),:);

%figure
%plot(OPTICAL_VELOCITY(:,1),OPTICAL_VELOCITY(:,2))
save RawOpticalVelocity.dat OPTICAL_VELOCITY

%%%%%%%%%%%%%%%%%%%%%%%%%%%%%%%%%%%%%%%%%%%%%%%%%%%%%%%%%%%%
```

```
%Fast Fourier Transform Filter
%%%%%%%%%%%%%%%%%%%%%%%%%%%%%%%%%%%%%%%%%%%%%%%%%%%%

%number of data points in optical velocity matrix
VELOCITY_POINTS=length(OPTICAL_VELOCITY);

%make the data periodic to prevent ringing
PERIODIC_VELOCITY = [OPTICAL_VELOCITY; flipud(OPTICAL_VELOCITY)];

%period of built periodic waveform
T=OPTICAL_VELOCITY(VELOCITY_POINTS,1);

%Returns the Fast Fourier Transform of each strain gauge.
FFT = fft(PERIODIC_VELOCITY(:,2));

%Corresponding frequencies returned by the indeces of the FFT terms
FREQ = 1/T;

%INDEX within FFT for Frequencys less than 60 secs.
%Takes into account that data set has been doubled
FFT_FREQ = 2*FREQ;

%Dummy filter to remove extraneous noise
%but retain the characteristic profile
%cut off frequencies higher than that of MIN_INDEX
%MIN_INDEX approximated by trial and error
MIN_INDEX=16;

FFT(MIN_INDEX:size(FFT,1)-MIN_INDEX,:)=0.0;

% Perform the Inverse Fast Fourier Transform on the data
I_FFT=ifft(FFT);

CLEAN_OPTICAL_VELOCITY=[OPTICAL_VELOCITY(:,1),real(I_FFT(1:VELOCITY_POIN
TS,:))];

%figure
%plot(CLEAN_OPTICAL_VELOCITY(:,1),CLEAN_OPTICAL_VELOCITY(:,2))

%%%%%%%%%%%%%%%%%%%%%%%%%%%%%%%%%%%%%%%%%%%%%%%%%%%%
%Linear interpolation of clean optical velocity data
%to make it the same size as Data, to facilitate
%numerical integration
%%%%%%%%%%%%%%%%%%%%%%%%%%%%%%%%%%%%%%%%%%%%%%%%%%%%

SLOPE=[];
LAST=0;
TEMP=[];
TEMP(:,1)=DATA(:,1);
j=1;
RUN=0;
RISE=0;

%Array of slopes used for linear interpolation
```

```
for i=1:(length(CLEAN_OPTICAL_VELOCITY)-1)
      SLOPE(i,1)=(CLEAN_OPTICAL_VELOCITY(i+1,2)-
CLEAN_OPTICAL_VELOCITY(i,2))/(CLEAN_OPTICAL_VELOCITY(i+1,1)-
CLEAN_OPTICAL_VELOCITY(i,1));
end

%Linear interpolation of clean optical velocity data into temp matrix
for i=1:length(DATA)

      %from start to end of optical velocity
      if (j<length(CLEAN_OPTICAL_VELOCITY))

            %If first optical velocity measurements do not correspond to
initial Data time
            if ((DATA(i,1)~=CLEAN_OPTICAL_VELOCITY(1,1)) & (LAST==0))
                  TEMP(i,2)=CLEAN_OPTICAL_VELOCITY(1,2);
            end

            %Interpolation between known optical velocities
            if (DATA(i,1)~=CLEAN_OPTICAL_VELOCITY(j,1) & (LAST>0))
                  RUN=TEMP(i,1)-TEMP(LAST,1);
                  RISE=RUN*SLOPE(j-1,1);
                  TEMP(i,2)=TEMP(LAST,2)+RISE;
            end

            %Copies over known optical velocities
            if (DATA(i,1)==CLEAN_OPTICAL_VELOCITY(j,1))
                  TEMP(i,2)=CLEAN_OPTICAL_VELOCITY(j,2);
                  j=j+1;
                  LAST=i;
            end

      end   %end if

      %from end of optical velocity to end of data
      if (j==length(CLEAN_OPTICAL_VELOCITY))
            TEMP(i,2)=CLEAN_OPTICAL_VELOCITY(j,2);
      end

end   %end for

INTERPOLATED_OPTICAL_VELOCITY=TEMP;


%%%%%%%%%%%%%%%%%%%%%%%%%%%%%%%%%%%%%%%%%%%%%
%Output Plots
%%%%%%%%%%%%%%%%%%%%%%%%%%%%%%%%%%%%%%%%%%%%%

figure
hold on
plot(CLEAN_OPTICAL_VELOCITY(:,1),CLEAN_OPTICAL_VELOCITY(:,2),"b");
plot(OPTICAL_VELOCITY(:,1),OPTICAL_VELOCITY(:,2),"g");
plot(OPTICAL_VELOCITY(:,1),(3.13+9.8*OPTICAL_VELOCITY(:,1)),"r");
title('Optical Velocity vs Time')
```

```
xlabel('Time (s)');
ylabel('Optical Velocity (m/s)');
legend('Filtered','Unfiltered','Expected Free Fall',3)
%axis([x1,x2,y1,y2])
%axis([0.07,0.12,2,2.9])
hold off

%%%%%%%%%%%%%%%%%%%%%%%%%%%%%%%%%%%%%%%%%%%%%%%%%%%%%%%%
%Save Processed Data as .dat File
%%%%%%%%%%%%%%%%%%%%%%%%%%%%%%%%%%%%%%%%%%%%%%%%%%%%%%%%

%save OpticalVelocity.dat INTERPOLATED_OPTICAL_VELOCITY

endfunction
```

This page intentionally left blank.

Annex B Pressed Notch Tip Dimensions

The following table shows measured dimensions of notch depth and notch tip angle for dynamic tear specimens used in this experiment. Not all specimens were measured. Blank cells correspond to unmeasured quantities.

Specimen	Measured Pressed Notch Depth	Measured Pressed Notch Tip Angle		Specimen	Measured Pressed Notch Depth	Measured Pressed Notch Tip Angle
AF1	0.302	42.5		**CW8**	0.2335	44
AF2	0.42			**DF4**	0.2215	39
AF3	0.16			**DF9**	0.245	43.5
AF4	0.15			**DW4**	0.2725	39
AF5	0.16			**DW8**	0.2805	42.5
AF6	0.15			**GF1**	0.274	43
AF7	0.14			**GF4**	0.256	39
AF8	0.14			**GW1**	0.251	41
AF9	0.15			**GW4**	0.3025	39
AW1	0.168	44		**A21**	0.245	39.5
AW2	0.197			**A22**	0.26	42.5
AW3	0.166			**A31**	0.38	41
AW4	0.131			**A32**	0.27	44.5
AW5	0.157	42		**A41**	0.25	41
AW6	0.171			**A42**	0.255	42.5
AW7	0.158			**A5**	0.245	42.5
AW8	0.149			**C21**	0.25	45
BF1	0.266			**C22**	0.26	43
BF5	0.259	41		**C31**	0.25	42.5
BW4	0.255			**C32**	0.245	41.5
BW8	0.2535			**C41**	0.235	42.5
CF4	0.281	42		**C42**	0.24	40
CF8	0.2795	43		**C5**	0.25	43
CW5	0.248	39				

This page intentionally left blank.

Annex C Dynamic Tear Test Results

The table below shows the results from the dynamic tear tests. Data for specimen type “D” was not recorded as it exhibited fully brittle fracture at room temperature. This is likely because of the large slag inclusion running through the fracture area of each specimen. A21 through A5 correspond to the “A” specimens notched on the fusion line. C21 through C5 correspond to the “C” specimens notched on the fusion line.

Specimen ID	Notch Location	Test Temperature (°C)	Dynamic Tear Energy (J)	Percent Shear Fracture (%)	Comment
AF1	F+1	20.1	1511.5	100	
AF2	F+1	-43.8	130.46	15	
AF3	F+1	-18	990.02	95	
AF4	F+1	-29.3	1056.9	95	
AF5	F+1	-29.3	491.27	50	
AF6	F+1	-29.3	353.86	30	
AF7	F+1	-20		60	failed optical velocity
AF8	F+1	-20	1024.4	95	
AF9	F+1	-10	1260.8	95	
AW1	W	20.8	1523.8	100	
AW2	W	-43.1	197.5	15	
AW3	W	-18.6	917.23	90	
AW4	W	-29.3	291.72	40	
AW5	W	-18.6	514.55	60	
AW6	W	-18.7	150	30	
AW7	W	-10	815.2	80	
AW8	W	0	1021.7	100	
BF1	F+1	20.9	1167.4	70	
BF2	F+1	-41.64	369.76	30	
BF3	F+1	-18.4	669.73	75	
BF4	F+1	-29.3	140.44	15	
BF5	F+1	-18.6	644.81	30	
BF6	F+1	-18.8	175	10	
BF7	F+1	-10	949.33	70	
BF8	F+1	-35	137.48	10	
BW1	W	21	1899.5	100	
BW2	W	-43	391.8	15	
BW3	W	-18.7	1515.9	100	
BW4	W	-29.3	532.53	30	
BW5	W	-18.8	476.14	20	
BW6	W	-18.7	1290.3	85	

BW7	W	-10	229.74	25	
BW8	W	0	334.09	35	slag inclusion
CF1	F+1	21.1	1794.4	100	
CF2	F+1	-43.4	422	55	
CF3	F+1	-18.4	927.95	90	
CF4	F+1	-29.1	765.92	85	
CF5	F+1	-10	1113.6	100	
CF6	F+1	-35	607.73	75	
CF7	F+1	0	1114.5	100	
CF8	F+1	-50	297.72	30	
CW1	W	21.2	1482.9	95	
CW2	W	-43.8	551.57	60	
CW3	W	-18.6	939.77	100	
CW4	W	-29.3	300.96	50	
CW5	W	-18.6	877.36	90	
CW6	W	-18.6	361.87	30	
CW7	W	-10	405.48	35	
CW8	W	0	1087.7	100	
DF1	F+1	21.2			slag inclusion
DF2	F+1				slag inclusion
DF3	F+1				slag inclusion
DF4	F+1				slag inclusion
DF5	F+1				slag inclusion
DF6	F+1				slag inclusion
DF7	F+1				slag inclusion
DF8	F+1				slag inclusion
DW1	W	21.2			slag inclusion
DW2	W				slag inclusion
DW3	W				slag inclusion
DW4	W				slag inclusion
DW5	W				slag inclusion
DW6	W				slag inclusion
DW7	W				slag inclusion
DW8	W				slag inclusion
GF1	F+1	21.7	822.65	100	
GF2	F+1	-42.7	464.66	90	
GF3	F+1	-18.25	617.61	100	
GF4	F+1	-29.3	650.01	100	
GF5	F+1	-50	388.66	85	
GF6	F+1	-60	321.86	75	
GF7	F+1	-70	107.55	20	
GW1	W	21.6	444.96	100	
GW2	W	-43.5	163.03	35	
GW3	W	-18.6	555.11	95	
GW4	W	-29.3	646.08	90	

GW5	W	-29.3		100	failed optical velocity
GW6	W	-29.3		100	failed optical velocity
GW7	W	-35	448.5	90	
A21	F	-10	729.81	78	
A22	F	0	1008.9	86	
A31	F	-30		20	failed to set trigger
A32	F	-20	591.66	58	
A41	F	-40	300.81	29	
A42	F	-10	1364.3	100	
A5	F	-20	708.66	66	
C21	F	23	1008.1	100	
C22	F	0	1050.9	100	
C31	F	-30	394.24	57	
C32	F	-20	480.1	58	
C41	F	-40	301.77	39	
C42	F	-10	371.71	41	
C5	F	-5	620	54	

C.1 Comparison of Absorbed Energy Measurement Methods

This table outlines the differences between absorbed energy calculated from conservation of kinetic and potential energy, and from integration of force vs. displacement data.

Dynamic Tear Energy (J)						
Specimen ID	**Notch Location**	**Test Temperature (°C)**	**Conservation of Energy**	**Integration of Force vs. Displacement**	**Absolute Difference (Conservation - Integration)**	**% Difference (Conservation - Integration) / Conservation**
AF1	F+1	20.1	1511.5	1178	333.5	22.06
AF2	F+1	-43.8	130.46	147	-16.54	-12.68
AF3	F+1	-18	990.02	799	191.02	19.29
AF4	F+1	-29.3	1056.9	788	268.9	25.44
AF5	F+1	-29.3	491.27	312	179.27	36.49
AF6	F+1	-29.3	353.86	238.3	115.56	32.66
AF7	F+1	-20	failed optical velocity		n/a	n/a
AF8	F+1	-20	1024.4	820.2	204.2	19.93
AF9	F+1	-10	1260.8	933.3	327.5	25.98
AW1	W	20.8	1523.8	1137	386.80	25.38
AW2	W	-43.1	197.5	148.6	48.90	24.76
AW3	W	-18.6	917.23	739.1	178.13	19.42
AW4	W	-29.3	291.72	233.4	58.32	19.99
AW5	W	-18.6	514.55	394.4	120.15	23.35
AW6	W	-18.7	150	114.8	35.20	23.47
AW7	W	-10	815.2	580.3	234.90	28.82
AW8	W	0	1021.7	808	213.70	20.92
BF1	F+1	20.9	1167.4	763	404.4	34.64

BF2	F+1	-41.64	369.76	217	152.76	41.31
BF3	F+1	-18.4	669.73	505	164.73	24.60
BF4	F+1	-29.3	140.44	82	58.44	41.61
BF5	F+1	-18.6	644.81	465	179.81	27.89
BF6	F+1	-18.8	175	51	124	70.86
BF7	F+1	-10	949.33	761	188.33	19.84
BF8	F+1	-35	137.48	59	78.48	57.08
BW1	W	21	1899.5	1323	576.50	30.35
BW2	W	-43	391.8	262	129.80	33.13
BW3	W	-18.7	1515.9	1238	277.90	18.33
BW4	W	-29.3	532.53	413	119.53	22.45
BW5	W	-18.8	476.14	331	145.14	30.48
BW6	W	-18.7	1290.3	910	380.30	29.47
BW7	W	-10	229.74	126	103.74	45.16
BW8	W	0	334.09	249	85.09	25.47
CF1	F+1	21.1	1794.4	1119	675.4	37.64
CF2	F+1	-43.4	422	349	73	17.30
CF3	F+1	-18.4	927.95	678	249.95	26.94
CF4	F+1	-29.1	765.92	559	206.92	27.02
CF5	F+1	-10	1113.6	886	227.6	20.44
CF6	F+1	-35	607.73	487	120.73	19.87
CF7	F+1	0	1114.5	867	247.5	22.21
CF8	F+1	-50	297.72	177	120.72	40.55
CW1	W	21.2	1482.9	907	575.90	38.84
CW2	W	-43.8	551.57	427	124.57	22.58
CW3	W	-18.6	939.77	726	213.77	22.75
CW4	W	-29.3	300.96	244	56.96	18.93
CW5	W	-18.6	877.36	669	208.36	23.75
CW6	W	-18.6	361.87	244	117.87	32.57
CW7	W	-10	405.48	292	113.48	27.99
CW8	W	0	1087.7	863	224.70	20.66
DF1	F+1	21.2		slag inclusion	n/a	n/a
DF2	F+1			slag inclusion	n/a	n/a
DF3	F+1			slag inclusion	n/a	n/a
DF4	F+1			slag inclusion	n/a	n/a
DF5	F+1			slag inclusion	n/a	n/a
DF6	F+1			slag inclusion	n/a	n/a
DF7	F+1			slag inclusion	n/a	n/a
DF8	F+1			slag inclusion	n/a	n/a
DW1	W	21.2		slag inclusion	n/a	n/a
DW2	W			slag inclusion	n/a	n/a
DW3	W			slag inclusion	n/a	n/a
DW4	W			slag inclusion	n/a	n/a
DW5	W			slag inclusion	n/a	n/a
DW6	W			slag inclusion	n/a	n/a
DW7	W			slag inclusion	n/a	n/a
DW8	W			slag inclusion	n/a	n/a
GF1	F+1	21.7	822.65	483	339.65	41.29
GF2	F+1	-42.7	464.66	359	105.66	22.74
GF3	F+1	-18.25	617.61	471	146.61	23.74
GF4	F+1	-29.3	650.01	515	135.01	20.77
GF5	F+1	-50	388.66	300	88.66	22.81
GF6	F+1	-60	321.86	266	55.86	17.36

GF7	F+1	-70	107.55	59	48.55	45.14
GW1	W	21.6	444.96	405	39.96	8.98
GW2	W	-43.5	163.03	95	68.03	41.73
GW3	W	-18.6	555.11	381	174.11	31.36
GW4	W	-29.3	646.08	519	127.08	19.67
GW5	W	-29.3	failed optical velocity		n/a	n/a
GW6	W	-29.3	failed optical velocity		n/a	n/a
GW7	W	-35	448.5	349	99.50	22.19
A21	F	-10	729.81	572	157.81	21.62
A22	F	0	1008.9	817	191.9	19.02
A31	F	-30	failed to set trigger		n/a	n/a
A32	F	-20	591.66	413	178.66	30.20
A41	F	-40	300.81	192	108.81	36.17
A42	F	-10	1364.3	1069	295.3	21.64
A5	F	-20	708.66	517	191.66	27.05
C21	F	23	1008.1	790	218.10	21.63
C22	F	0	1050.9	827	223.90	21.31
C31	F	-30	394.24	297	97.24	24.67
C32	F	-20	480.1	409	71.10	14.81
C41	F	-40	301.77	238	63.77	21.13
C42	F	-10	371.71	293	78.71	21.18
C5	F	-5	620	464	156.00	25.16

This page intentionally left blank.

Distribution list

Document No.: DRDC Atlantic TM 2010-220

LIST PART 1: Internal Distribution by Centre

4 DRDC Atlantic Dockyard Laboratory Pacific (3 Hardcopies, 1 CD)

1 DRDC Atlantic (Attn: A. Nolting)

3 DRDC Atlantic Library (1 Hardcopy, 2 CDs)

8 TOTAL LIST PART 1

LIST PART 2: External Distribution by DRDKIM

1 Library and Archives Canada, Attn: Military Archivist, Governments Records Branch

1 DMSS 2-3-4 Materials and Welding Engineer (Attn: Dr. J. Huang)
LSTL, 555 blvd de la Carriere, 5-WB06
NDHQ – 101 Colonel By Dr
Ottawa, ON K1A 0K2

1 DRDKIM

3 TOTAL LIST PART 2

11 TOTAL COPIES REQUIRED

This page intentionally left blank.

DOCUMENT CONTROL DATA

(Security classification of title, body of abstract and indexing annotation must be entered when the overall document is classified)

1. ORIGINATOR (The name and address of the organization preparing the document. Organizations for whom the document was prepared, e.g. Centre sponsoring a contractor's report, or tasking agency, are entered in section 8.)

Defence R&D Canada – Atlantic
9 Grove Street
P.O. Box 1012
Dartmouth, Nova Scotia B2Y 3Z7

2. SECURITY CLASSIFICATION (Overall security classification of the document including special warning terms if applicable.)

UNCLASSIFIED

3. TITLE (The complete document title as indicated on the title page. Its classification should be indicated by the appropriate abbreviation (S, C or U) in parentheses after the title.)

Ductile to Brittle Transition Behaviour of HSLA-65 Steel Welds: Dynamic Tear Testing

4. AUTHORS (last name, followed by initials – ranks, titles, etc. not to be used)

Aucoin, N.M.

5. DATE OF PUBLICATION (Month and year of publication of document.)	6a. NO. OF PAGES (Total containing information, including Annexes, Appendices, etc.)	6b. NO. OF REFS (Total cited in document.)
January 2011	58	8

7. DESCRIPTIVE NOTES (The category of the document, e.g. technical report, technical note or memorandum. If appropriate, enter the type of report, e.g. interim, progress, summary, annual or final. Give the inclusive dates when a specific reporting period is covered.)

Technical Memorandum

8. SPONSORING ACTIVITY (The name of the department project office or laboratory sponsoring the research and development – include address.)

Defence R&D Canada – Atlantic
9 Grove Street
P.O. Box 1012
Dartmouth, Nova Scotia B2Y 3Z7

9a. PROJECT OR GRANT NO. (If appropriate, the applicable research and development project or grant number under which the document was written. Please specify whether project or grant.)	9b. CONTRACT NO. (If appropriate, the applicable number under which the document was written.)
11gu05	

10a. ORIGINATOR'S DOCUMENT NUMBER (The official document number by which the document is identified by the originating activity. This number must be unique to this document.)	10b. OTHER DOCUMENT NO(s). (Any other numbers which may be assigned this document either by the originator or by the sponsor.)
DRDC Atlantic TM 2010-220	

11. DOCUMENT AVAILABILITY (Any limitations on further dissemination of the document, other than those imposed by security classification.)

Unlimited

12. DOCUMENT ANNOUNCEMENT (Any limitation to the bibliographic announcement of this document. This will normally correspond to the Document Availability (11). However, where further distribution (beyond the audience specified in (11) is possible, a wider announcement audience may be selected.))

Unlimited

13. ABSTRACT (A brief and factual summary of the document. It may also appear elsewhere in the body of the document itself. It is highly desirable that the abstract of classified documents be unclassified. Each paragraph of the abstract shall begin with an indication of the security classification of the information in the paragraph (unless the document itself is unclassified) represented as (S), (C), (R), or (U). It is not necessary to include here abstracts in both official languages unless the text is bilingual.)

HSLA-65 steel (ASTM A945, grade 65 [1]) is regarded as an excellent naval ship steel. The use of this steel in future naval platforms, which may be required to serve in Arctic conditions, requires a detailed knowledge of the steel's low temperature mechanical properties, particularly when the steel is welded. A previous study on the transition temperature, conducted by Bayley and Mantei [2], showed that the transition temperature was significantly higher than the requirement of -40°C in the heat affected zone of flux-cored arc welding (FCAW) welds.

The current study re-examines the transition behaviour of HSLA-65 welds using dynamic tear testing, where specimens are significantly larger than in Charpy tests and could more accurately predict the behaviour of large scale structures. The current study also examines an alternate approach for determining the energy absorbed during a dynamic tear test using the integral definition of work.

The results of this study show that transition temperatures determined through dynamic tear testing are much higher than those determined through Charpy impact testing. Several areas of each weld were tested. In all cases, the fusion line of the weld was found to have the highest transition temperature, the heat affected zone was found to have the lowest transition temperature, and the weld metal fell somewhere in between. Based on a transition temperature requirement of less than -40°C, none of the welds tested was found to be fit for service in Arctic conditions.

14. KEYWORDS, DESCRIPTORS or IDENTIFIERS (Technically meaningful terms or short phrases that characterize a document and could be helpful in cataloguing the document. They should be selected so that no security classification is required. Identifiers, such as equipment model designation, trade name, military project code name, geographic location may also be included. If possible keywords should be selected from a published thesaurus, e.g. Thesaurus of Engineering and Scientific Terms (TEST) and that thesaurus identified. If it is not possible to select indexing terms which are Unclassified, the classification of each should be indicated as with the title.)

ASTM E604; ASTM A945; Dynamic Tear Test; Ductile-Brittle Transition; Welded HSLA-65; Charpy

This page intentionally left blank.

Defence R&D Canada

Canada's leader in defence
and National Security
Science and Technology

R & D pour la défense Canada

Chef de file au Canada en matière
de science et de technologie pour
la défense et la sécurité nationale

www.drdc-rddc.gc.ca